



24 **I. Introduction.** Secondary organic aerosol (SOA) particles make up a substantial  
25 fraction of tropospheric aerosol and are known to lead to negative radiative forcing,<sup>1-3</sup> yet,  
26 their formation ranks among the least understood processes in the atmosphere.<sup>1,4-7</sup> Many  
27 studies<sup>2,4,8-13</sup> support the idea that the gas-phase oxidation products of biogenic volatile  
28 compounds can either a) partition to existing particles due to reduced volatility compared  
29 to the parent compounds or b) dissolve in aerosol or cloud water and participate in  
30 aqueous phase reactions to form low-volatility material. Surface tension is expected to be  
31 of particular importance for SOA formation and growth as it involves processes occurring  
32 at the interface between the SOA particle phase and the gas phase.<sup>14,15</sup> Moreover,  
33 atmospheric particles, once formed, can contain thousands of organic compounds or  
34 surfactants that can decrease the surface tension and thereby change aerosol particle  
35 properties such as cloud droplet formation, reactivity, and ice nucleation.<sup>16-21</sup> Specifically,  
36 it has been reported that organic surfactants can influence the propensity of atmospheric  
37 aerosol particles to act as cloud condensation nuclei (CCN) by depressing the surface  
38 tension at the moment of activation.<sup>22-30</sup> Lower surface tension values result in decreases  
39 in the water vapor supersaturation required for cloud droplet activation, depending on  
40 ionic content, pH, temperature, and meteorological conditions. McNeill and coworkers  
41 recently showed that volatile surfactant species such as methylglyoxal and acetaldehyde  
42 can suppress surface tension at the gas-aerosol interface beyond predictions based on  
43 bulk surface tension measurements, leading to significantly enhanced CCN activity.<sup>28</sup>  
44 Chemical reactions at the surface and in the bulk of the particle between aerosol  
45 components may also influence overall surface tension and thus impact the dependence

46 of CCN activity on the presence of surfactants. Yet, surface tension effects of many  
47 compounds relevant for SOA particle formation remain largely uncharacterized.<sup>17,31</sup>  
48 Given their importance for global SOA particle formation,<sup>2,32,33</sup> we report here surface  
49 tension values, measured using pendant drop tensiometry, of suspended drops of  
50 deionized water and 1.0 M ammonium sulfate solutions containing 0.1 to 30 mM  
51 concentrations of synthetically prepared isoprene-derived SOA particle constituents.  
52 Specifically, we studied the isoprene oxidation products  $\alpha$ -,  $\delta$ - and *cis*- and *trans*- $\beta$ -  
53 isoprene epoxide (IEPOX) (1–4, Figure 1), and *syn*- and *anti*-2-methyltetraol (5, 6). We  
54 are motivated by a recent study by Wennberg and coworkers reporting that *cis*- $\beta$ -IEPOX  
55 (2) and *trans*- $\beta$ -IEPOX (1) are produced in much higher yield than  $\alpha$ -IEPOX (4) during  
56 isoprene oxidation by hydroxyl radicals with a ratio of  $\alpha$ -IEPOX (4) to *cis*- $\beta$ -IEPOX (2)  
57 to *trans*- $\beta$ -IEPOX (1) of 1:20.5:27.9.<sup>34</sup> The  $\delta$ -IEPOX (3) isomer was not detected in this  
58 study. We report octanol-water partitioning coefficients ( $K_{ow}$ ) and viscosities of the  
59 compounds under investigation. These studies reveal that  $\alpha$ -IEPOX (4) significantly  
60 decreases surface tension in water (19% at 30 mM) and in 1.0 M  $(\text{NH}_4)_2\text{SO}_4$  (30% at 30  
61 mM). The *trans*- $\beta$ -IEPOX (1) isomer also decreases surface tension substantially with an  
62 overall decrease of 15% in water and in 1.0 M  $(\text{NH}_4)_2\text{SO}_4$  at a concentration of 30 mM.  
63 Surface tension results indicate that these compounds may enhance aerosol CCN activity  
64 although further studies will be necessary to verify this experimentally.

## 65 **II. Experimental.**

66 **II.A. Synthesis of Isoprene-derived SOA Particle Precursors.** Synthesis of all  
67 compounds studied here are described in previous work.<sup>35</sup> The alkene diol (7) was  
68 prepared in order to examine the impact of the epoxide functional group on  $K_{ow}$  values.

69 Purity of synthesized compounds was determined based on NMR spectra. Surface tension  
70 measurements performed in this work are most likely insensitive to impurities below the  
71 detection limit of NMR spectroscopy due to the higher concentrations of IEPOX and  
72 tetraols used in this study (above micromolar amounts).

73 **II.B. Partition Experiments.** The octanol water partition coefficient,  $K_{ow}$ , was  
74 determined gas-chromatographically after thorough mixing of the two phases to reach the  
75 equilibrium using the shake flask method (mass-balance approach). For the IEPOX (1–4)  
76 and alkene diol (7) compounds, stock solutions (~45 mM) were prepared in high purity  
77 analytical grade 1-octanol (Sigma Aldrich) presaturated with water. Equal volumes of  
78 stock solutions and deionized water were mixed in three separate 15 mL propylene  
79 conical tubes. Due to the limited solubility of the 2-methyltetraol compounds in octanol,  
80 stock solutions (~45 mM) of the tetraol compounds were prepared in deionized water.  
81 Equal volumes of stock solution and 1-octanol presaturated with water were mixed in  
82 three separate 15 mL polypropylene conical tubes. In all cases, phases of the solvent  
83 systems were mutually saturated by shaking for ~24 hours on a mechanical shaker at  
84 room temperature. The three mixtures for each compound were subsequently centrifuged  
85 for 5 minutes at 3000 rpm to ensure complete phase separation. Three aliquots of the  
86 octanol phase were taken to determine the concentration of the IEPOX compounds (1–4),  
87 the tetraols (5, 6) and the alkene diol (7) compound.

88 The concentration of the compounds from the octanol phase for the epoxides and tetraols  
89 were determined using an Agilent 5973 gas chromatograph-mass spectrometer with a  
90 FFAP column (length 30 m, inner diameter 0.25 mm, film thickness 0.25  $\mu$ m) and a  
91 quadrupole analyzer and EI ionization. The injector and detector temperatures were

92 260°C and 250°C respectively. For the alkene diol and IEPOX compounds, the oven had  
93 an initial temperature of 40°C and a final temperature of 200°C with a ramp rate of  
94 15°C/min. For the tetraol compounds, the oven had an initial temperature of 150°C and a  
95 final temperature of 220°C with a ramp rate of 30°C/min. The gas flow rate was 1.0  
96 mL/min.

97 For IEPOX and alkene diol compounds, the quantity of the compound present at  
98 equilibrium in the aqueous phase was calculated from difference between the quantity of  
99 the compound originally introduced and the quantity in the octanol phase determined  
100 using the mass balance technique.

101 **II.C. Viscosity Studies.** All viscosities were measured using solutions of 0.325 g/mL of  
102 the compound of interest and 0.1625 g/mL  $(\text{NH}_4)_2\text{SO}_4$ . Viscosity measurements are  
103 relative to a control solution (0.1625 g/mL  $(\text{NH}_4)_2\text{SO}_4$  in deionized  $\text{H}_2\text{O}$ ) and were  
104 determined using a technique similar to a Cannon-Fenske viscometer, by measuring the  
105 time taken for the solutions to pass through a 1 mL plastic syringe as reported by McNeill  
106 and Drozd.<sup>36</sup>

107 **II.D. Dynamic Surface Tension Measurements.** Pendant drop tensiometry (PDT) was  
108 used to measure surface tension over time for all solutions in this study on a FTA125  
109 goniometer. Solutions were prepared in  $\text{dH}_2\text{O}$  or with 1.0 M  $(\text{NH}_4)_2\text{SO}_4$ . The pH of  
110 solutions containing  $(\text{NH}_4)_2\text{SO}_4$  ranged from approximately 5.0 to 6.0 while pH ranged  
111 from approximately 6.0 to 7.0 in  $\text{dH}_2\text{O}$ . All solutions fell within the bounds of  
112 atmospherically relevant pH for aerosols in the troposphere (pH 0-8).<sup>37,38</sup> Solutions  
113 containing 100 mM IEPOX compounds in 1 M  $(\text{NH}_4)_2\text{SO}_4$  were allowed to stir at room  
114 temperature for one week and monitored by NMR. No conversion into the organosulfate

115 or tetraols was observed during this time. All solutions for surface tension experiments  
116 were measured within a week of their formation and were stored in glass vials at  $\sim 4^\circ\text{C}$  in  
117 between measurements in order to further reduce the probability of conversion of IEPOX  
118 compounds into the organosulfate or tetraol products. Concentrations of compounds in  
119 solutions ranged from 0-30 mM although in some cases higher concentrations (50 mM,  
120 100 mM) were also analyzed. All surface tension experiments were performed at ambient  
121 temperature and pressure. Relative humidity ranged from 15% to 45%, and the laboratory  
122 temperature ranged from  $20^\circ\text{C}$  to  $23^\circ\text{C}$ .

123 Droplets of sample solutions were formed at the tip of a flat stainless steel needle 1 mL  
124 syringe mounted on the instrument and inserted  $\sim 1$  cm into a quartz cuvette containing  
125 0.5 mL of  $\text{dH}_2\text{O}$ . All droplets were approximately  $7\ \mu\text{L}$  in volume and varied between 2.1  
126 and 2.4 mm in diameter. After formation, the droplet was allowed to stabilize and images  
127 were captured  $\sim 5$  seconds after droplet formation. Images were taken every 0.3 seconds  
128 for 10 minutes, resulting in 1500 images for each experiment and measurements were  
129 repeated 5-7 times for each solution. Recent dynamic surface tension studies using the  
130 extracted total surfactant component of the PM10 size fraction of aerosol particles  
131 collected in an urban setting reported similar equilibration times.<sup>39</sup> Surface tension for  
132 each image was determined by fitting the shape of the drop to the Young-Laplace  
133 equation, which relates interfacial tension to drop shape as described by Adamson and  
134 Gast.<sup>40</sup>

$$135 \quad \Delta\rho gh = \gamma \left( \frac{1}{R_1} + \frac{1}{R_2} \right) \quad (1)$$

136 where  $\Delta\rho$  is the difference in densities of the drop and the surrounding media,  $g$  is  
137 acceleration due to gravity,  $h$  is the height generally measured from the apex of the drop,  
138  $\gamma$  is the surface tension and  $R_1$  and  $R_2$  are the radii of curvature. To calculate the surface  
139 tension of the drop, images were captured using a RS170 CCD camera equipped with a  
140 microscope lens. FTA32 v2.0 software fit each drop profile and determined distances  
141 analytically. A regression then obtains the best overall fit to the Laplace-Young equation  
142 with the fitting parameter being interfacial tension with units of mN/m.

### 143 **III. Results and Discussion**

144 **III.A. Partitioning and Viscosity Studies.** The octanol water partition coefficient,  $K_{ow}$ ,  
145 is defined as the ratio between the concentrations of a compound of interest in octanol to  
146 the one in water once equilibrium is established.<sup>41</sup> Experimental values of  $K_{ow}$  serve as a  
147 measure of hydrophobicity while also allowing for the prediction of other physical values  
148 relevant to cloud formation that can be more difficult to experimentally measure.<sup>42-44</sup>  
149 Since particles can undergo liquid-liquid phase separation and often contain an aqueous  
150 and an organic-rich phase,<sup>45</sup>  $K_{ow}$  values indicate the phase these compounds will  
151 preferentially partition to. Our gas-chromatographically determined  $K_{ow}$  values are listed  
152 in Figure 1.

153 In general,  $K_{ow}$  values followed the expected trends in hydrophobicity for each of the  
154 compounds. The *trans*- and *cis*- $\beta$ -IEPOX compounds 1 and 2 were found to have the  
155 most negative  $K_{ow}$  values, which is consistent with the presence of two primary hydroxyl  
156 groups. These compounds also displayed the longest GC retention times (~16.5 min) with  
157 nearly identical fragmentation patterns (Figure S1).  $\delta$ -IEPOX (3), with its secondary and  
158 primary hydroxyl groups, had a slightly higher partition coefficient.  $\alpha$ -IEPOX (4) proved

159 to be the most hydrophobic epoxide with the least negative  $K_{ow}$  value of all the epoxides.  
160 These results are consistent with  $\alpha$ -IEPOX (4) having the least accessible hydroxyl  
161 groups of the epoxides due to the placement of the methyl group and possibly indicate  
162 that  $\alpha$ -IEPOX (4) would be the isomer most likely to partition into the organic-rich phase  
163 of particles. Replacement of the epoxide group in  $\alpha$ -IEPOX (4) with a simple alkene (7)  
164 shifted the  $\log(K_{ow})$  upward by about 0.4 units. This demonstrates that removal of the  
165 polar epoxide group significantly increases hydrophobicity.

166 The exact  $K_{ow}$  values of the two tetraol diastereomers (5 and 6) could not be determined,  
167 possibly due to their very limited solubility in octanol. GC traces of the octanol fraction  
168 in tetraol partitioning experiments showed that concentrations of the tetraols in the  
169 octanol fractions were below the detection limit. This indicates that the  $\log(K_{ow})$  values  
170 for tetraol compounds 5 and 6 would be much more negative than the values found for  
171 the IEPOX compounds.

172 Relative viscosities are listed in Figure 1. The substances tested are all viscous liquids  
173 from room temperature down to  $-40$  °C. The epoxides (1–3) have a viscosity similar to  
174 glycerol ( $1.98 \pm 0.03$ ), whereas the 2-methyltetraols (5, 6) are slightly more viscous and  
175 almost gelatinous.

176 **III.B. Dynamic Surface Tension Measurements.** Based on the relevance of surface  
177 tension measurements in the prediction of new particle formation and aerosol CCN  
178 properties, the effect of concentration on surface tension over time was measured for the  
179 four epoxide isomers (1–4) and the two tetraol diastereomers (5, 6) in  $dH_2O$  and in 1.0 M  
180  $(NH_4)_2SO_4$ . As shown in Fig. 2, results in  $dH_2O$  showed that the  $\alpha$ -IEPOX (4) is by far  
181 the most surface active of the epoxide compounds. At the highest concentration measured



182 (30 mM), interfacial tension for  $\alpha$ -IEPOX (4) was lowered by 5% at  $t=0$  seconds and  
183 decreased an additional 14% over the course of 10 minutes relative to  $\text{dH}_2\text{O}$ . While some  
184 of this decrease may be due to evaporation, the majority of the effect is most likely due to  
185 the migration of  $\alpha$ -IEPOX (4) to the surface of the droplet. Based on partitioning  
186 coefficients,  $\alpha$ -IEPOX (4) is the most hydrophobic of the epoxides and therefore would  
187 be more likely to partition from the bulk of the aqueous droplet to the surface.

188 As shown in Fig. 3, the surface tension lowering effect of  $\alpha$ -IEPOX (4) was greatly  
189 enhanced by the presence of 1.0 M  $(\text{NH}_4)_2\text{SO}_4$ . The presence of 1.0 M  $(\text{NH}_4)_2\text{SO}_4$  in  
190 water raises the surface tension of the droplets by approximately 3%. Addition of 30 mM  
191  $\alpha$ -IEPOX (4) to the 1.0 M  $(\text{NH}_4)_2\text{SO}_4$  solution prompted a 20% drop in surface tension at  
192  $t=0$  seconds and decreased an additional 10% over the course of 10 minutes (resulting in  
193 an overall 30% decrease compared to interfacial tension of  $\text{dH}_2\text{O}$ ). The presence of  
194 inorganic salt most likely decreased the solubility of  $\alpha$ -IEPOX (4) in water, increasing  
195 the concentration of  $\alpha$ -IEPOX (4) at the surface of the droplet due to “salting out”. These  
196 types of nonreactive salt-organic interactions may have a significant influence of surface  
197 tension of atmospheric aerosols.<sup>46-50</sup> *Trans*- $\beta$ -IEPOX (1) also demonstrated significant  
198 surface activity. However, addition of 1.0 M  $(\text{NH}_4)_2\text{SO}_4$  did not appear to greatly enhance  
199 these surface tension lowering effects. Both with and without inorganic salt, a solution of  
200 30 mM *trans*- $\beta$ -IEPOX (1) resulted in an overall decrease of 15% in surface tension  
201 relative to  $\text{dH}_2\text{O}$  after 10 minutes.  $\delta$ -IEPOX (3) and *cis*- $\beta$ -IEPOX (2) both showed  
202 minimal surface tension-lowering effects. A more concentrated solution of 100 mM  $\delta$ -  
203 IEPOX (3) was required in order to achieve the 15% surface tension depression seen for  
204 the 30 mM *trans*- $\beta$ -IEPOX (1) solution. Addition of 1.0 M  $(\text{NH}_4)_2\text{SO}_4$  also did not appear

205 to greatly enhance the surface tension lowering effects of either  $\delta$ -IEPOX (3) or *cis*- $\beta$ -  
206 IEPOX (2).

207 Regarding the tetraols, Fig. 4 shows a sharp drop in surface activity between 20 mM and  
208 10 mM *anti*-2-methyltetraol (6) solutions in dH<sub>2</sub>O. Specifically, *anti*-2-methyltetraol (6)  
209 showed surface activity comparable to *trans*- $\beta$ -IEPOX (1) at 30 mM in dH<sub>2</sub>O. The *syn*-2-  
210 methyltetraol (5) showed less surface activity compared to the *anti*-2-methyltetraol (6)  
211 but did exhibit a similar increase in surface activity between the 20 mM and 10 mM  
212 solutions in dH<sub>2</sub>O. This phenomenon was also observed for the *anti*-2-methyltetraol (6) in  
213 1.0 M (NH<sub>4</sub>)<sub>2</sub>SO<sub>4</sub> solutions but was less pronounced for the *syn*-2-methyltetraol (5) under  
214 the same conditions. This result could be an indication of the increased solubility of the  
215 2-methyltetraol diastereomers in water and therefore a smaller concentration of the 2-  
216 methyltetraols at the surface of the droplet. We conclude that the 2-methyltetraol  
217 diastereomers may be completely soluble with little effect on droplet surface tension until  
218 a critical concentration above 10 mM is reached.

219 Droplets of pure water and 1.0 M (NH<sub>4</sub>)<sub>2</sub>SO<sub>4</sub> were also exposed to the vapor pressure  
220 over neat IEPOX compounds, however, no change in the surface tension of the droplets  
221 was observed on a timescale of twenty minutes. We caution here that the partial pressure  
222 of IEPOX used in these experiments was much higher than its typical pressure in the  
223 atmosphere, and that gas and particle phase diffusion limitations for this experiment  
224 would also differ for submicron-sized aerosol particles: a recent chamber study of  
225 methylglyoxal demonstrated enhanced CCN activity for ammonium sulfate aerosols  
226 exposed to methylglyoxal and/or acetaldehyde over 3-5 hours, but not when exposure  
227 occurred in an aerosol flow tube on a timescale of seconds or minutes.<sup>28</sup>

228 Taken together, our surface tension and partitioning studies reveal that  $\alpha$ -IEPOX (4) is  
229 both the most hydrophobic and most surface active of all the compounds studied.  
230 However, there does not appear to be a consistent correlation between  
231 hydrophobicity/viscosity and surface activity of the compounds studied here. For  
232 example, *cis*- $\beta$ -IEPOX (2) and *trans*- $\beta$ -IEPOX (1) were found to possess nearly identical  
233  $K_{ow}$  values and therefore similar levels of hydrophobicity but *trans*- $\beta$ -IEPOX (1)  
234 demonstrated greater surface activity relative to *cis*- $\beta$ -IEPOX (2). The difference in  
235 surface activity of *trans*- $\beta$ -IEPOX (1) and *cis*- $\beta$ -IEPOX (2) may be a reflection of the  
236 different relative orientations of the two hydroxyl and the single epoxide groups in *cis*-  
237 and *trans*- $\beta$ -IEPOX (1, 2) as well as the difference in their propensity to form hydrogen  
238 bonds with water molecules inside the water droplet. The greater surface tension  
239 depression of *trans*- $\beta$ -IEPOX (1) may indicate that this compound forms fewer hydrogen  
240 bonds than *cis*- $\beta$ -IEPOX (2), which could be verified through computational chemistry,  
241 such as molecular dynamics simulations.”

242 **IV. Implications for Atmospheric Chemistry.** Experimental and field studies have  
243 shown that surface tension depression by organic compounds is a critical component of  
244 predicting aerosol particle behavior.<sup>15,19-21,26,51-61</sup> These studies have demonstrated that the  
245 amount of solute present in an aerosol particle (known as the dry diameter) as well as the  
246 surface tension of the droplet can alter its propensity to act as a cloud condensation  
247 nucleus. Köhler theory describes cloud droplet activation and growth from soluble  
248 particles.<sup>62,63</sup> The Köhler curve is given by:

249 
$$s = \frac{A}{D_p} - \frac{B}{D_p^3} \quad (2)$$

250 with

251 
$$A = \frac{4M_w\sigma}{RT\rho_w} \quad \text{and} \quad B = \frac{6n_sM_w}{\pi\rho_w} \quad (3)$$

252 where  $s$  is the supersaturation,  $D_p$  is the diameter of the aqueous droplet,  $M_w$  is the  
253 molecular of water and  $\rho_w$  its density,  $R$  is the gas constant,  $T$  is temperature,  $\sigma$  is surface  
254 tension, and  $n_s$  is the number of moles of solute. A decrease in surface tension due to the  
255 presence of surfactants would therefore decrease parameter  $A$  and result in increased  
256 CCN activation. If the bulk solute content of the particle remains constant, the effect of  
257 organic surfactants on equilibrium CCN activity can be assumed to be purely surface  
258 tension based. This assumption is valid based on the fact that gas-phase isoprene  
259 oxidation products will be continuously taken up at the gas-aerosol interface as they are  
260 consumed in heterogeneous reactions within the bulk and at the surface of the aerosol.<sup>49</sup>  
261 Using this assumption, the critical supersaturation for particles of a given size can be  
262 described as follows:

263 
$$s_c^* = \left( \frac{\sigma}{\sigma_w} \right)^{3/2} s_c \quad (4)$$

264 Here,  $s_c^*$  is the critical supersaturation,  $\sigma_w$  and  $\sigma$  are the surface tension of water and the  
265 particle, respectively, and  $s_c$  is the critical supersaturation of particle with the surface  
266 tension of water (72.8 mN/m).<sup>64</sup> For all IEPOX and 2-methyltetraol compounds, dynamic  
267 surface tension measurements were fit to exponential curves in order to determine the  
268 equilibrium surface tension at  $t=\infty$  (Table 1). The equilibrium surface tension was used in  
269 Eq. 4 to calculate the critical supersaturation ratio ( $s_c^*/s_c$ ), which are listed in Table 2.

270 While there is some uncertainty regarding the in-particle concentrations of IEPOX and its  
271 reaction products, we can make reasonable estimates of these values based on field and

272 modeling studies. Chan et al.<sup>65</sup> reported up to 24 ng m<sup>-3</sup> of IEPOX in Yorkville, GA  
273 during the 2008 August Mini-Intensive Gas and Aerosol Study (AMIGAS). During that  
274 period, they also measured 33.4 mg m<sup>-3</sup> of PM<sub>2.5</sub>. Therefore, the observed IEPOX loading  
275 corresponds to an in-particle concentration of ~7 mM, assuming 1.2 g cm<sup>-3</sup> for the  
276 particle density. The McNeill group's coupled gas-aqueous aerosol chemistry model,  
277 Gas Aerosol Model for Mechanism Analysis (GAMMA),<sup>66</sup> has been updated to include  
278 the latest aqueous phase IEPOX chemistry and physical parameters.<sup>67</sup> GAMMA 1.4  
279 simulations predict in-particle concentrations of unreacted IEPOX between 2 and 23 mM  
280 in a rural scenario (see Supporting Information). Therefore, we take here 7.5 mM as an  
281 example of an atmospherically relevant IEPOX in-particle concentration and find that  $\alpha$ -  
282 IEPOX (4) exhibited the largest decrease in  $s_c^*/s_c$  (9%), with an even larger decrease  
283 observed (23%) in 1.0 M (NH<sub>4</sub>)<sub>2</sub>SO<sub>4</sub>. *Trans*- $\beta$ -IEPOX (1) was also observed to lower  
284 surface tension and therefore is also expected to lead to decreased supersaturation ratios  
285 and enhanced CCN activity. The potential of *trans*- $\beta$ -IEPOX to enhance CCN activity is  
286 particularly significant based on recent studies demonstrating that *trans*- $\beta$ -IEPOX is the  
287 most abundantly produced isomer relative to other IEPOX isomers during isoprene  
288 oxidation.<sup>34</sup> At 10 mM,  $s_c^*/s_c$  for *trans*- $\beta$ -IEPOX (1) is predicted to decrease by 8% in  
289 dH<sub>2</sub>O and in (NH<sub>4</sub>)<sub>2</sub>SO<sub>4</sub>. Surface tension depression, and therefore the predicted impact  
290 on CCN activity, was less significant for *cis*- $\beta$ -IEPOX (2),  $\delta$ -IEPOX (3) and the 2-  
291 methyltetraols (5, 6). On a per-mole basis, surface tension depression by *trans*- $\beta$ -IEPOX  
292 is similar to that observed for methylglyoxal in bulk solutions.<sup>49</sup> The Henry's Law  
293 constant for IEPOX is several orders of magnitude higher than that of methylglyoxal,<sup>67</sup>  
294 leading to a greater potential for suppression of aerosol surface tension by these species

295 via bulk effects. That being said, as demonstrated by McNeill and coworkers,<sup>28</sup> bulk  
296 absorption of surface-active gases is apparently not a requirement for surface tension  
297 depression and enhanced CCN activity. In fact, while reactive uptake may be important  
298 in other systems, and is certainly important for SOA particles, it is not relevant for our  
299 aqueous model experiments, as complementary NMR studies discussed in the Supporting  
300 Information show no hydrolysis of the epoxides in ammonium sulfate solution over the  
301 course of one week. Our results thus set the stage for future investigations of the effects  
302 of *trans*- $\beta$ -IEPOX on the CCN activity of aqueous aerosols.

303 **V. Conclusions.** In conclusion, we report dynamic surface tension measurements, using  
304 pendant drop tensiometry, of synthetically prepared isoprene-derived SOA particle  
305 constituents. Specifically, we studied the isoprene oxidation products  $\alpha$ -,  $\delta$ - and *cis*- and  
306 *trans*- $\beta$ -isoprene epoxide (IEPOX) (1–4) and *syn*- and *anti*-2-methyltetraol (5, 6)  
307 compounds. In addition, we experimentally determined octanol-water partitioning  
308 coefficients ( $K_{ow}$ ) and viscosities of these compounds. Results these experiments revealed  
309 that  $\alpha$ -IEPOX (4) is the most hydrophobic and surface active of the compounds studied  
310 here, however the hydrophobicity of these compounds did not coincide with surface  
311 activity for all compounds. Calculation of supersaturation ratios from surface tension  
312 values demonstrated that *trans*- $\beta$ -IEPOX (1) lowers supersaturation ratios significantly  
313 while the largest decrease in supersaturation ratios was calculated for  $\alpha$ -IEPOX (4).  
314 Other compounds measured, *cis*- $\beta$ -IEPOX (2),  $\delta$ -IEPOX (3), and the 2-methyltetraols (5,  
315 6), demonstrated less significant surface activity and therefore minimal decreases in  
316 supersaturation ratios at higher concentrations.

317 The enhanced surface activity of *trans*- $\beta$ -IEPOX (1) and its potential to significantly  
318 decrease supersaturation ratios is particularly important based on its correlation with  
319 recent sum frequency generation (SFG) spectroscopy studies towards the identification of  
320 molecular constituents on the surfaces of isoprene-derived SOA particles.<sup>35</sup> This surface  
321 specific study identified *trans*- $\beta$ -IEPOX (1) as the closest match to the SFG spectra of  
322 isoprene-derived SOA surfaces, which coupled with surface tension experiments  
323 presented here, strongly indicates that *trans*- $\beta$ -IEPOX (1) may be present in higher  
324 concentrations at the surface of aerosol particles relative to other IEPOX isomers. This  
325 conclusion is also supported by the study by Wennberg and coworkers where *trans*- $\beta$ -  
326 IEPOX (1) was found to be produced in higher yields relative to other IEPOX isomers  
327 during isoprene oxidation by hydroxyl radicals. Reactive uptake of IEPOX compounds  
328 into aerosol particles by acid-catalyzed epoxide ring opening can also lead to formation  
329 of organosulfate and organonitrate derivatives<sup>68-70</sup> so future studies will involve  
330 synthesizing these derivatives and analyzing their surface activity and other  
331 atmospherically relevant properties.

332 **VI. Acknowledgments.** MAU gratefully acknowledges support from a NASA Earth and  
333 Space Fellowship. This work was supported by the Initiative for Sustainability and  
334 Energy at Northwestern (ISEN) and the National Science Foundation (NSF)  
335 Environmental Chemical Sciences Program in the Division of Chemistry under Grant No.  
336 1212692.

337

338

339

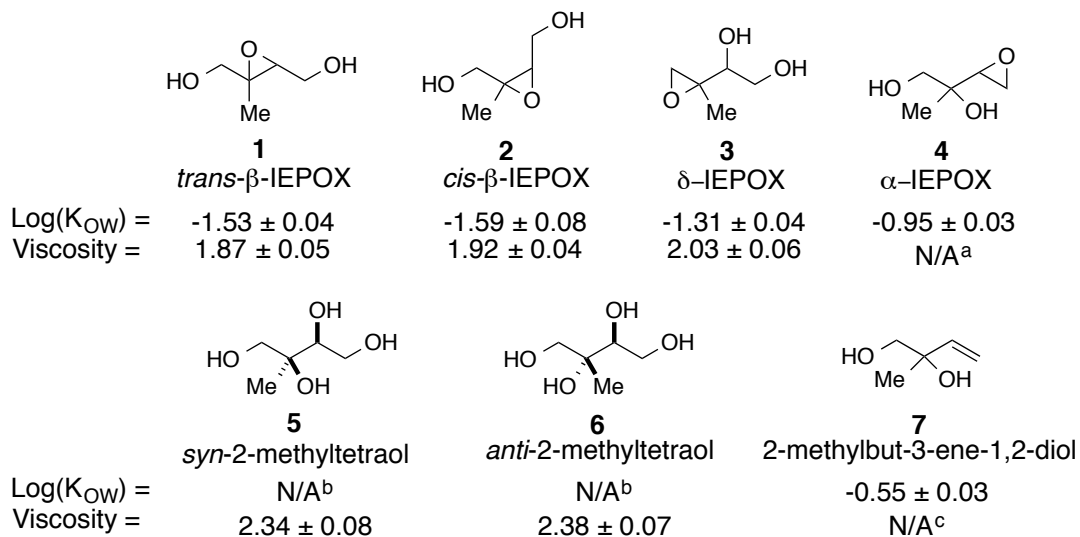
340

341

342

343

344



a.  $\alpha$ -IEPOX (4) was insoluble in dH<sub>2</sub>O at higher concentrations used for viscosity experiments b. 2-methyltetraols (5,6) had concentrations in octanol below the detection limit c. Viscosity for alkene diol (7) was not measured due to its increased hydrophobicity relative to  $\alpha$ -IEPOX (4) observed during partitioning experiments.

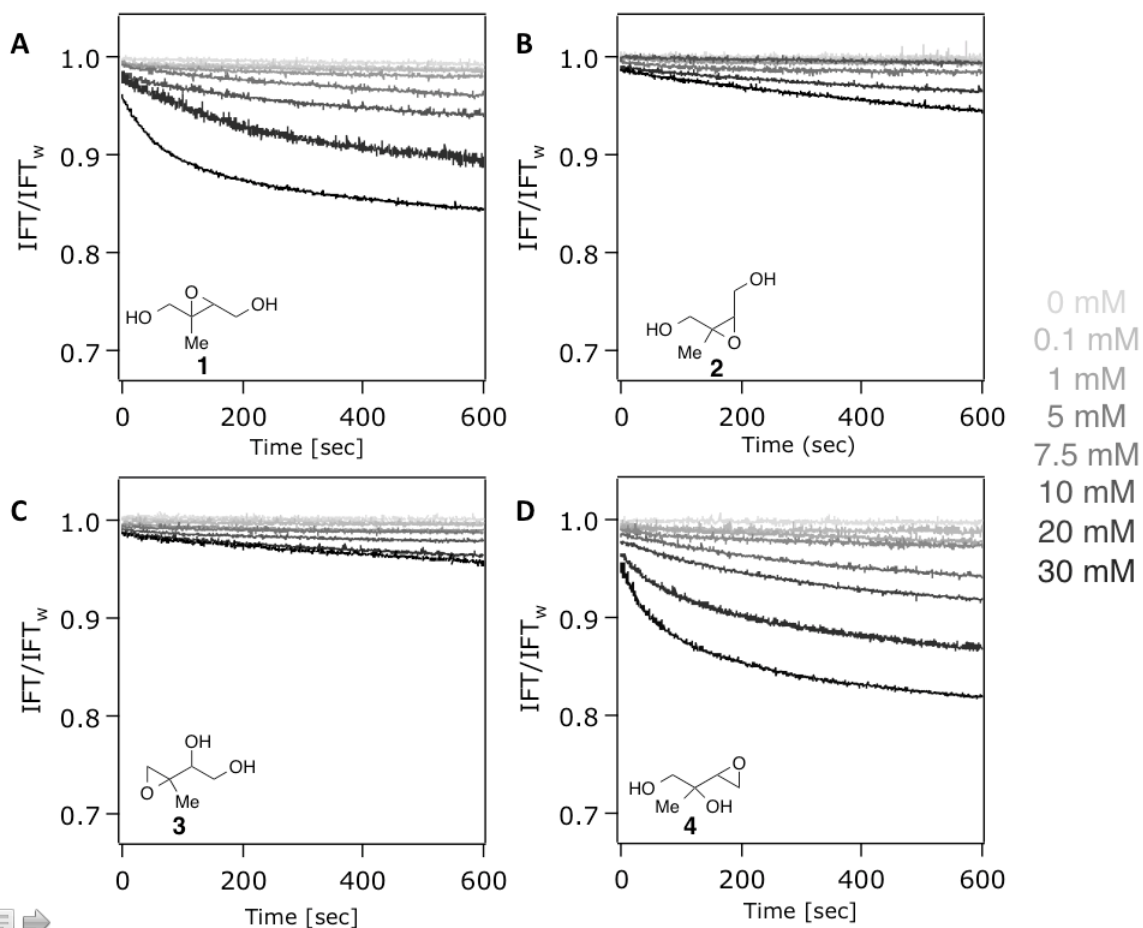
345

346 **Figure 1.** Octanol-water partition coefficients and viscosity values for epoxides 1–4 and

347 tetraols 5 and 6.

348

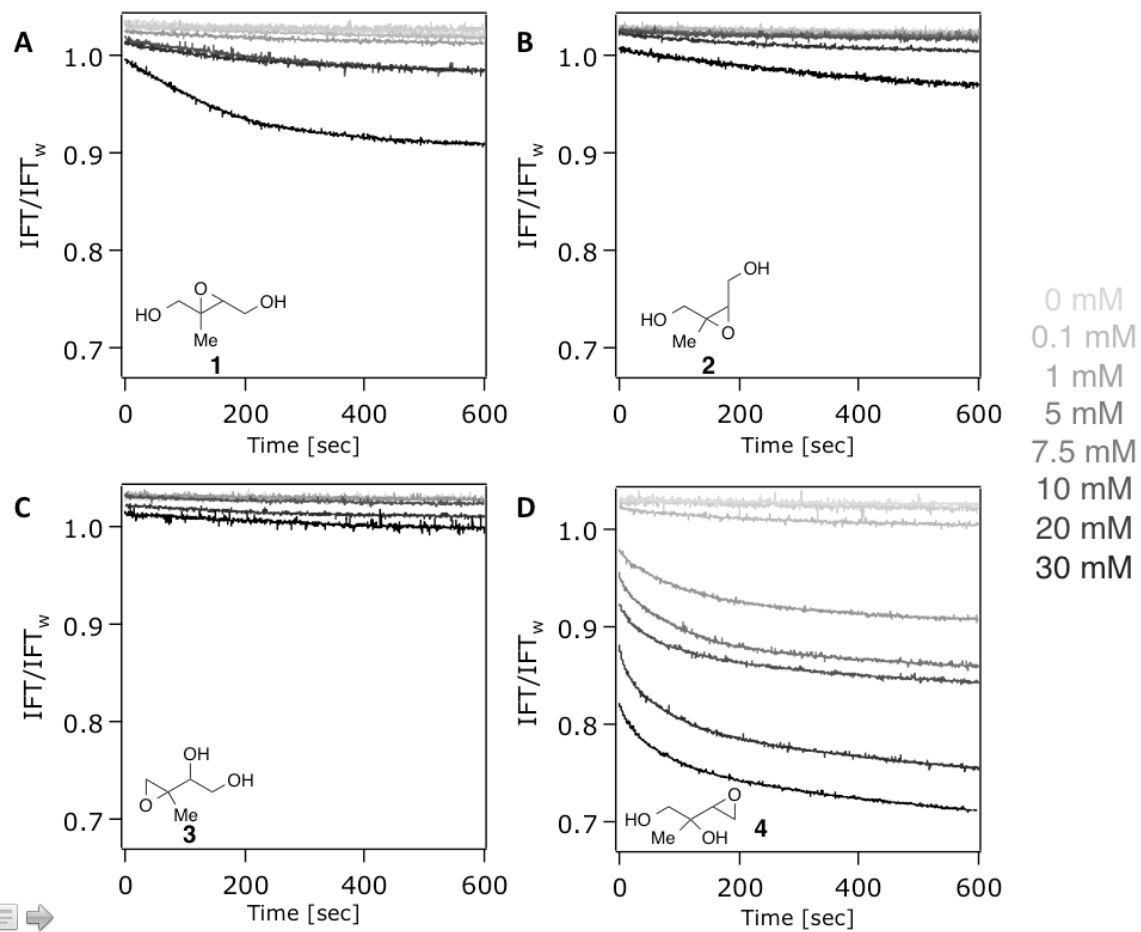




349  
350  
351  
352



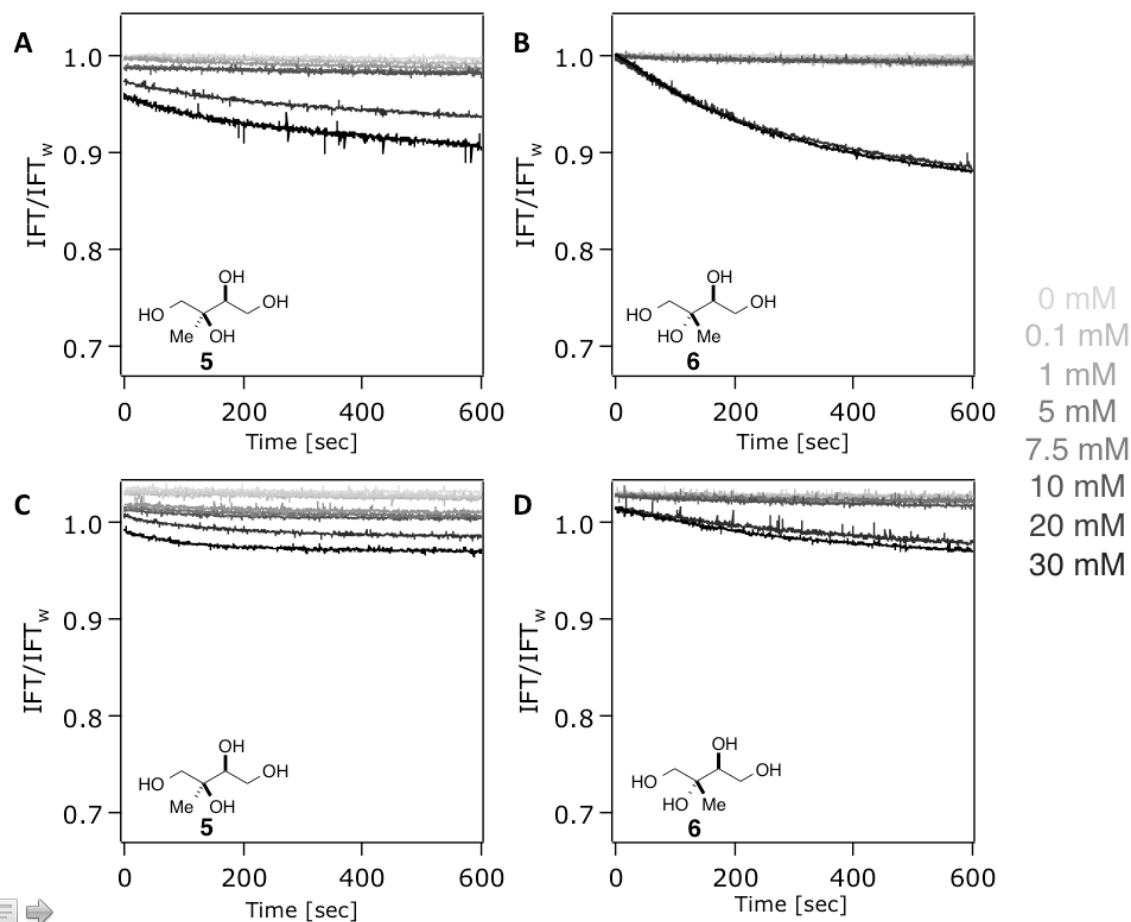
**Figure 2.** Dynamic surface tension measurements for IEPOX compounds in dH<sub>2</sub>O. A) trans-β-IEPOX (1) B) cis-β-IEPOX (2) C) δ-IEPOX (3) D) α-IEPOX (4).



353  
354  
355  
356



**Figure 3.** Dynamic surface tension measurements for IEPOX compounds in 1 M  $(\text{NH}_4)_2\text{SO}_4$ . A) trans- $\beta$ -IEPOX (1) B) cis- $\beta$ -IEPOX (2) C)  $\delta$ -IEPOX (3) D)  $\alpha$ -IEPOX (4).



357



358

**Figure 4.** Dynamic surface tension measurements for 2-methyltetraol in

359

dH<sub>2</sub>O (A and B) and 1 M (NH<sub>4</sub>)<sub>2</sub>SO<sub>4</sub> (C and D). A/C) syn-2-methyltetraol (5) B/D) anti-

360

2-methyltetraol (6).

361

362

363

364

365

366

367

368

369

370 **Table 1.** Equilibrium surface tension (at  $t=\infty$ ) for IEPOX (1–4) and 2-methyltetraols (5,6).

Concentration (mM)	1	2	3	4	5	6
0	71.8 (73.87)	72.73 (74.38)	72.84 (74.85)	72.4 (74.59)	72.48 (75.01)	72.47 (74.67)
0.1	71.4 (74.63)	72.59 (74.28)	72.3 (74.63)	71.96 (74.0)	72.06 (74.54)	72.36 (74.69)
1	71.68 (73.81)	72.31 (74.25)	72.46 (74.4)	70.7 (73.01)	71.8 (74.2)	71.30 (74.72)
5	71.20 (73.56)	72.32 (74.17)	71.96 (74.80)	70.69 (66.09)	71.68 (73.47)	71.70 (74.27)
7.5	68.72 (73.49)	71.67 (74.14)	71.85 (74.32)	67.64 (62.70)	71.48 (73.18)	71.27 (74.37)
10	67.87 (71.11)	71.7 (74.00)	71.09 (74.39)	65.95 (61.45)	71.1 (73.09)	71.34 (73.74)
20	64.57 (71.39)	69.01 (72.93)	69.31 (73.46)	62.99 (55.14)	67.78 (71.72)	61.45 (70.36)
30	61.62 (65.89)	65.5 (69.21)	67.4 (72.09)	59.46 (51.89)	65.35 (70.64)	60.96 (69.97)

a. Surface tension values at  $t=\infty$  for solutions of IEPOX (1–4) and 2-methyltetraols (5, 6) in dH<sub>2</sub>O based on exponential fits. All values have units of mN/m. b. Values in parentheses denote surface tension values in 1 M (NH<sub>4</sub>)<sub>2</sub>SO<sub>4</sub>. c. Error in exponential fit varied from 0.01-0.2 for IEPOX 1-3 and *syn*-2-methyltetraol 5, 0.01-0.1 for IEPOX 4, and from 0.01-0.06 for *anti*-2-methyltetraol 6.

371

372

373 **Table 2.** Supersaturation ratios for IEPOX (1–4) and 2-methyltetraols (5, 6).

Concentration (mM)	1	2	3	4	5	6
0	1.0 (1.02)	1.00 (1.0)	1.00 (1.04)	1.0 (1.04)	0.99 (1.05)	0.99 (1.04)
0.1	1.0 (1.04)	1.00 (1.03)	1.0 (1.04)	0.98 (1.0)	0.99 (1.0)	0.99 (1.04)
1	0.98 (1.02)	0.99 (1.03)	0.99 (1.0)	0.9 (1.00)	1.0 (1.0)	0.97 (1.04)
5	0.97 (1.02)	0.99 (1.03)	0.98 (1.04)	0.96 (0.86)	0.98 (1.01)	0.98 (1.03)
7.5	0.92 (1.01)	0.98 (1.03)	0.98 (1.03)	0.90 (0.80)	0.97 (1.00)	0.97 (1.03)
10	0.90 (0.96)	1.0 (1.02)	0.96 (1.03)	0.86 (0.78)	1.0 (1.00)	0.97 (1.02)
20	0.84 (0.97)	0.9 (1.00)	0.93 (1.01)	0.80 (0.66)	0.90 (0.98)	0.78 (0.95)
30	0.78 (0.86)	0.9 (0.93)	0.9 (1.0)	0.74 (0.60)	0.85 (0.96)	0.77 (0.94)

a. Supersaturation ratios ( $s^*/s_c$ ) for solutions of IEPOX (1–4) and 2-methyltetraols (5, 6) in dH<sub>2</sub>O. b. Values in parentheses denote supersaturation ratios ( $s^*/s_c$ ) in 1 M (NH<sub>4</sub>)<sub>2</sub>SO<sub>4</sub>. Errors in ratios varied from 0.01-0.2 for IEPOX 1-3 and *syn*-2-methyltetraol 5, 0.01-0.1 for IEPOX 4, and 0.01-0.09 for *anti*-2-methyltetraol 6.

374

375

376

377

378

379

380

381

382

383

384 **References.**

- 385 (1) Kanakidou, M.; Seinfeld, J. H.; Pandis, S. N.; Barnes, I.; Dentener, F. J.;  
386 Facchini, M. C.; Van Dingenen, R.; Ervens, B.; Nenes, A.; Nielsen, C. J.; Swietlicki, E.;  
387 Putaud, J. P.; Balkanski, Y.; Fuzzi, S.; Horth, J.; Moortgat, G. K.; Winterhalter, R.;  
388 Myhre, C. E. L.; Tsigaridis, K.; Vignati, E.; Stephanou, E. G.; Wilson, J. *Atmos Chem*  
389 *Phys* **2005**, *5*, 1053.
- 390 (2) Carlton, A. G.; Wiedinmyer, C.; Kroll, J. H. *Atmos Chem Phys* **2009**, *9*,  
391 4987.
- 392 (3) Williams, J.; Crowley, J.; Fischer, H.; Harder, H.; Martinez, M.; Petäjä,  
393 T.; Rinne, J.; Bäck, J.; Boy, M.; Dal Maso, M.; Hakala, J.; Kajos, M.; Keronen, P.;  
394 Rantala, P.; Aalto, J.; Aaltonen, H.; Paatero, J.; Vesala, T.; Hakola, H.; Levula, J.; Pohja,  
395 T.; Herrmann, F.; Auld, J.; Mesarchaki, E.; Song, W.; Yassaa, N.; Nölscher, A.; Johnson,  
396 A. M.; Custer, T.; Sinha, V.; Thieser, J.; Pouvesle, N.; Taraborrelli, D.; Tang, M. J.;  
397 Bozem, H.; Hosaynali-Beygi, Z.; Axinte, R.; Oswald, R.; Novelli, A.; Kubistin, D.; Hens,  
398 K.; Javed, U.; Trawny, K.; Breitenberger, C.; Hidalgo, P. J.; Ebben, C. J.; Geiger, F. M.;  
399 Corrigan, A. L.; Russell, L. M.; Ouwersloot, H. G.; Vilà-Guerau de Arellano, J.;  
400 Ganzeveld, L.; Vogel, A.; Beck, M.; Bayerle, A.; Kampf, C. J.; Bertelmann, M.; Köllner,  
401 F.; Hoffmann, T.; Valverde, J.; González, D.; Riekkola, M. L.; Kulmala, M.; Lelieveld, J.  
402 *Atmos Chem Phys* **2011**, *11*, 10599.
- 403 (4) Hallquist, M.; Wenger, J. C.; Baltensperger, U.; Rudich, Y.; Simpson, D.;  
404 Claeys, M.; Dommen, J.; Donahue, N. M.; George, C.; Goldstein, A. H.; Hamilton, J. F.;  
405 Herrmann, H.; Hoffmann, T.; Iinuma, Y.; Jang, M.; Jenkin, M. E.; Jimenez, J. L.;  
406 Kiendler-Scharr, A.; Maenhaut, W.; McFiggans, G.; Mentel, T. F.; Monod, A.; Prevot, A.  
407 S. H.; Seinfeld, J. H.; Surratt, J. D.; Szmigielski, R.; Wildt, J. *Atmos Chem Phys* **2009**, *9*,  
408 5155.
- 409 (5) Goldstein, A. H.; Galbally, I. E. *Environ Sci Technol* **2007**, *41*, 1514.
- 410 (6) Galbally, I. E.; Lawson, S. J.; Weeks, I. A.; Bentley, S. T.; Gillett, R. W.;  
411 Meyer, M.; Goldstein, A. H. *Environ Chem* **2007**, *4*, 178.
- 412 (7) Riipinen, I.; Pierce, J. R.; Yli-Juuti, T.; Nieminen, T.; Häkkinen, S.; Ehn,  
413 M.; Junninen, H.; Lehtipalo, K.; Petäjä, T.; Slowik, J.; Chang, R.; Shantz, N. C.; Abbatt,  
414 J.; Leaitch, W. R.; Kerminen, V. M.; Worsnop, D. R.; Pandis, S. N.; Donahue, N. M.;  
415 Kulmala, M. *Atmos Chem Phys* **2011**, *11*, 3865.
- 416 (8) Kroll, J. H.; Seinfeld, J. H. *Atmos Environ* **2008**, *42*, 3593.
- 417 (9) Lin, Y. H.; Zhang, Z. F.; Docherty, K. S.; Zhang, H. F.; Budisulistiorini, S.  
418 H.; Rubitschun, C. L.; Shaw, S. L.; Knipping, E. M.; Edgerton, E. S.; Kleindienst, T. E.;  
419 Gold, A.; Surratt, J. D. *Environ Sci Technol* **2012**, *46*, 250.
- 420 (10) Worton, D. R.; Surratt, J. D.; Lafranchi, B. W.; Chan, A. W.; Zhao, Y.;  
421 Weber, R. J.; Park, J. H.; Gilman, J. B.; de Gouw, J.; Park, C.; Schade, G.; Beaver, M.;  
422 Clair, J. M.; Crouse, J.; Wennberg, P.; Wolfe, G. M.; Harrold, S.; Thornton, J. A.;  
423 Farmer, D. K.; Docherty, K. S.; Cubison, M. J.; Jimenez, J. L.; Frossard, A. A.; Russell,  
424 L. M.; Kristensen, K.; Glasius, M.; Mao, J.; Ren, X.; Brune, W.; Browne, E. C.; Pusede,  
425 S. E.; Cohen, R. C.; Seinfeld, J. H.; Goldstein, A. H. *Environ Sci Technol* **2013**, *47*,  
426 11403.
- 427 (11) Kourtev, I.; Fuller, S. J.; Giorio, C.; Healy, R. M.; Wilson, E.; O'Connor,  
428 I.; Wenger, J. C.; McLeod, M.; Aalto, J.; Ruuskanen, T. M.; Maenhaut, W.; Jones, R.;

- 429 Venables, D. S.; Sodeau, J. R.; Kulmala, M.; Kalberer, M. *Atmos Chem Phys* **2014**, *14*,  
430 2155.
- 431 (12) Ehn, M.; Thornton, J. A.; Kleist, E.; Sipila, M.; Junninen, H.; Pullinen, I.;  
432 Springer, M.; Rubach, F.; Tillmann, R.; Lee, B.; Lopez-Hilfiker, F.; Andres, S.; Acir, I.  
433 H.; Rissanen, M.; Jokinen, T.; Schobesberger, S.; Kangasluoma, J.; Kontkanen, J.;  
434 Nieminen, T.; Kurten, T.; Nielsen, L. B.; Jorgensen, S.; Kjaergaard, H. G.; Canagaratna,  
435 M.; Maso, M. D.; Berndt, T.; Petaja, T.; Wahner, A.; Kerminen, V. M.; Kulmala, M.;  
436 Worsnop, D. R.; Wildt, J.; Mentel, T. F. *Nature* **2014**, *506*, 476.
- 437 (13) Claeys, M.; Wang, W.; Ion, A. C.; Kourtchev, I.; Gelencsér, A.; Maenhaut,  
438 W. *Atmos Environ* **2004**, *38*, 4093.
- 439 (14) Wang, J.; Wexler, A. S. *Geophys Res Lett* **2013**, *40*, 2834.
- 440 (15) Djikae, Y. S.; Tabazadeh, A. *Journal of Geophysical Research* **2003**, *108*,  
441 4689.
- 442 (16) Schwier, A. N.; Viglione, G. A.; Li, Z.; Faye McNeill, V. *Atmos Chem*  
443 *Phys* **2013**, *13*, 10721.
- 444 (17) McNeill, V. F.; Sareen, N.; Schwier, A. N. *Top. Curr. Chem.* **2014**, *339*,  
445 201.
- 446 (18) Aumann, E.; Tabazadeh, A. *Journal of Geophysical Research* **2008**, *113*,  
447 D23205.
- 448 (19) Tabazadeh, A. *Atmos Environ* **2005**, *39*, 5472.
- 449 (20) Taraniuk, I.; Graber, E. R.; Kostinski, A.; Rudich, Y. *Geophys Res Lett*  
450 **2007**, *34*, L16807.
- 451 (21) Taraniuk, I.; Kostinski, A. B.; Rudich, Y. *Geophys Res Lett* **2008**, *35*,  
452 L19810.
- 453 (22) Facchini, M. C.; Mircea, M.; Fuzzi, S.; Charlson, R. J. *Nature* **1999**, *401*,  
454 257.
- 455 (23) Kiss, G.; Tombacz, E.; Hansson, H. C. *J Atmos Chem* **2005**, *50*, 279.
- 456 (24) Shulman, M. L.; Jacobson, M. C.; Carlson, R. J.; Synovec, R. E.; Young,  
457 T. E. *Geophys Res Lett* **1996**, *23*, 277.
- 458 (25) Asa-Awuku, A.; Sullivan, A. P.; Hennigan, C. J.; Weber, R. J.; Nenes, A.  
459 *Atmos Chem Phys* **2008**, *8*, 799.
- 460 (26) Facchini, M. C.; Decesari, S.; Mircea, M.; Fuzzi, S.; Loglio, G. *Atmos*  
461 *Environ* **2000**, *34*, 4853.
- 462 (27) Novakov, T.; Penner, J. E. *Nature* **1993**, *365*, 823.
- 463 (28) Sareen, N.; Schwier, A. N.; Lathem, T. L.; Nenes, A.; McNeill, V. F.  
464 *Proceedings of the National Academy of Sciences of the United States of America* **2013**,  
465 *110*, 2723.
- 466 (29) Salma, I.; Ocskay, R.; Varga, I.; Maenhaut, W. *Journal of Geophysical*  
467 *Research* **2006**, *111*, 205.
- 468 (30) Hitzenberger, R.; Berner, A.; Kasper-Giebl, A.; Loflund, M.; Puxbaum, H.  
469 *Journal of Geophysical Research* **2002**, *107*, 4752.
- 470 (31) Woo, J. L.; Kim, D. D.; Schwier, A. N.; Li, R.; McNeill, V. F. *Faraday*  
471 *Discuss.* **2013**, *165*, 357.
- 472 (32) Paulot, F.; Crouse, J. D.; Kjaergaard, H. G.; Kurten, A.; St Clair, J. M.;  
473 Seinfeld, J. H.; Wennberg, P. O. *Science* **2009**, *325*, 730.

- 474 (33) Claeys, M.; Graham, B.; Vas, G.; Wang, W.; Vermeylen, R.; Pashynska,  
475 V.; Cafmeyer, J.; Guyon, P.; Andreae, M. O.; Artaxo, P.; Maenhaut, W. *Science* **2004**,  
476 *303*, 1173.
- 477 (34) Bates, K. H.; Crounse, J. D.; St Clair, J. M.; Bennett, N. B.; Nguyen, T.  
478 B.; Seinfeld, J. H.; Stoltz, B. M.; Wennberg, P. O. *J Phys Chem A* **2014**, *118*, 1237.
- 479 (35) Ebben, C. J.; Strick, B. F.; Upshur, M. A.; Chase, H. M.; Achtyl, J. L.;  
480 Thomson, R. J.; Geiger, F. M. *Atmos Chem Phys* **2014**, *14*, 2303.
- 481 (36) Drozd, G. T.; McNeill, V. F. *Environ. Sci. Process Impacts* **2014**, *16*, 741.
- 482 (37) Keene, W. C. *Journal of Geophysical Research* **2004**, *109*.
- 483 (38) Zhang, Q.; Jimenez, J. L.; Worsnop, D. R.; Canagaratna, M. *Environ Sci*  
484 *Technol* **2007**, *41*, 3213.
- 485 (39) Noziere, B.; Baduel, C.; Jaffrezo, J. L. *Nature communications* **2014**, *5*,  
486 3335.
- 487 (40) Adamson, A. W.; Gast, A. P. *Physical Chemistry of Surfaces*; 6th ed. ed.;  
488 John Wiley & Sons, Inc.: New York, 1997.
- 489 (41) Leo, A.; Hansch, C.; Elkins, D. *Chem. Rev.* **1971**, *71*, 525.
- 490 (42) Finizio, A.; Mackay, D.; Bidleman, T.; Harner, T. *Atmos Environ* **1997**, *31*,  
491 2289.
- 492 (43) Klopffer, W.; Rippen, G.; Frische, R. *Ecotoxicol. Environ. Saf.* **1982**, *6*,  
493 294.
- 494 (44) Meylan, W. M.; Howard, P. H. *Chemosphere* **2005**, *61*, 640.
- 495 (45) Yuan, Y.; Renbaum-Wolff, L.; Carreras-Sospedra, M.; Hanna, S. J.;  
496 Hiranuma, N.; Kamal, S.; Smith, M. L.; Zhang, X.; Weber, R. J.; Shilling, J. E.; Dabdub,  
497 D.; Martin, S. T.; Bertram, A. K. *Proceedings of the National Academy of Sciences of the*  
498 *United States of America* **2012**, *109*, 13188.
- 499 (46) Li, Z.; Williams, A. L.; Rood, M. J. *J. Atmos. Sci.* **1998**, *55*, 1859.
- 500 (47) Matijevic, E.; Pethica, B. A. *Trans. Faraday Soc.* **1958**, *54*, 1383.
- 501 (48) Schwier, A.; Mitroo, D.; McNeill, V. F. *Atmos Environ* **2012**, *54*, 490.
- 502 (49) Sareen, N.; Schwier, A. N.; Shapiro, E. L.; Mitroo, D.; McNeill, V. F.  
503 *Atmos Chem Phys* **2010**, *10*, 997.
- 504 (50) Li, Z.; Schwier, A. N.; Sareen, N.; McNeill, V. F. *Atmos Chem Phys* **2011**,  
505 *11*, 11617.
- 506 (51) Cruz, C. N.; Pandis, S. N. *Journal of Geophysical Research* **1998**, *103*,  
507 13111.
- 508 (52) Ekstrom, S.; Noziere, B.; Hansson, H. C. *Atmos Chem Phys* **2009**, *9*, 973.
- 509 (53) Corrigan, C. E.; Novakov, T. *Atmos Environ* **1999**, *33*, 2661.
- 510 (54) Cruz, C. N.; Pandis, S. N. *Atmos Environ* **1997**, *31*, 2205.
- 511 (55) Henning, S.; Rosenorn, T.; D'Anna, B.; Gola, A. A.; Svenningsson, B.;  
512 Bilde, M. *Atmos Chem Phys* **2005**, *5*, 575.
- 513 (56) Prenni, A. J.; DeMott, P. J.; Kreidenweis, S. M.; Sherman, D. E. *J Phys*  
514 *Chem A* **2001**, *105*, 11240.
- 515 (57) Raymond, T. M. *Journal of Geophysical Research* **2003**, *108*, 4469.
- 516 (58) Raymond, T. M. *Journal of Geophysical Research* **2002**, *107*, 4787.
- 517 (59) Liu, P. S. K.; Leitch, W. R.; Banic, C. M.; Li, S. M.; Ngo, D.; Megaw, W.  
518 J. *Journal of Geophysical Research* **1996**, *101*, 28971.

- 519 (60) Broekhuizen, K.; Kumar, P. P.; Abbatt, J. P. D. *Geophys Res Lett* **2004**, *31*,  
520 107.
- 521 (61) Kumar, P. P.; Broekhuizen, K.; Abbatt, J. P. D. *Atmos Chem Phys* **2003**, *3*,  
522 509.
- 523 (62) Kohler, H. *Trans. Faraday Soc.* **1936**, *32*, 1152.
- 524 (63) Seinfeld, J. H.; Pandis, S. N. *Atmospheric Chemistry and Physics: from*  
525 *air pollution to climate change*; Wiley: New York, 1998.
- 526 (64) Engelhart, G. J.; Asa-Awuku, A.; Nenes, A.; Pandis, S. N. *Atmos Chem*  
527 *Phys* **2008**, *8*, 3937.
- 528 (65) Chan, M. N.; Surratt, J. D.; Claeys, M.; Edgerton, E. S.; Tanner, R. L.;  
529 Shaw, S. L.; Zheng, M.; Knipping, E. M.; Eddingsaas, N. C.; Wennberg, P. O.; Seinfeld,  
530 J. H. *Environmental Science & Technology* **2010**, *44*, 4590.
- 531 (66) McNeill, V. F.; Woo, J. L.; Kim, D. D.; Schwier, A. N.; Wannell, N. J.;  
532 Sumner, A. J.; Barakat, J. M. *Env. Sci. Technol.* **2012**, *46*, 8075.
- 533 (67) Nguyen, T. B.; Coggon, M. M.; Bates, K. H.; Zhang, X.; Schwantes, R.  
534 H.; Schilling, K. A.; Loza, C. L.; Flagan, R. C.; Wennberg, P. O.; Seinfeld, J. H. *Atmos*  
535 *Chem Phys* **2014**, *14*, 3497.
- 536 (68) Surratt, J. D.; Kroll, J. H.; Kleindienst, T. E.; Edney, E. O.; Claeys, M.;  
537 Sorooshian, A.; Ng, N. L.; Offenberg, J. H.; Lewandowski, M.; Jaoui, M.; Flagan, R. C.;  
538 Seinfeld, J. H. *Environ Sci Technol* **2007**, *41*, 517.
- 539 (69) Surratt, J. D.; Chan, A. W.; Eddingsaas, N. C.; Chan, M.; Loza, C. L.;  
540 Kwan, A. J.; Hersey, S. P.; Flagan, R. C.; Wennberg, P. O.; Seinfeld, J. H. *Proceedings*  
541 *of the National Academy of Sciences of the United States of America* **2010**, *107*, 6640.
- 542 (70) Darer, A. I.; Cole-Filipiak, N. C.; O'Connor, A. E.; Elrod, M. J. *Environ*  
543 *Sci Technol* **2011**, *45*, 1895.  
544  
545